https://doi.org/10.5194/hess-2021-174
Preprint. Discussion started: 30 March 2021

Hydrology and Earth System Sciences
Discussions

Exploring the role of soil storage capacity for explaining deviations from the Budyko curve using a simple water balance model

Jan Bondy[1], Jan Wienhöfer[1], Laurent Pfister[2], Erwin Zehe[1]

[1] Institute of Water Resources and River Basin Management, Karlsruhe Institute of Technology – KIT, Karlsruhe, Germany
[2] Luxembourg Institute of Science and Technology, Environmental Research and Innovation Department, Catchment and Eco-hydrology Group, Belvaux, Luxembourg

Correspondence to: Jan Bondy (jan.bondy@kit.edu)

Abstract.

The Budyko curve is a widely used framework for predicting the steady-state water balance –solely based on the hydro-climatic setting of river basins. While this framework has been tested and verified across a wide range of climates and settings around the globe, numerous catchments have been reported to considerably deviate from the predicted behavior. Here, we hypothesize that storage capacity and field capacity of the root zone are important controls of the water limitation of evapotranspiration and thus deviations of the mean annual water balance from the Budyko curve. For testing our hypothesis, we selected 16 catchments of different climatic settings and varied the corresponding parameters of a simple water balance model that was previously calibrated against long-term data and investigated the corresponding variations of the simulated water balance in the Budyko space. We found that total soil storage capacity –by controlling water availability and limitation of evapotranspiration– explains deviations of the evaporation ratio (EVR) from the Budyko curve. Similarly, however to a lesser extent, the evaporation ratio showed sensitivity to alterations of the field capacity. In most cases, the parameter variations generated evaporation ratios enveloping the Budyko curve. The distinct soil storage volumes that matched the Budyko curve clustered at a normalized storage capacity equivalent to 5-15 % of mean annual precipitation. The second, capillarity-related soil parameter clustered at around 0.6-0.8, which is in line with its hydropedological interpretation. A simultaneous variation of both parameters provided additional insights into the interrelation of both parameters and their joint control on offsets from the Budyko curve. Here we found three different sensitivity patterns and we conclude the study with a reflection relating these offsets to the concept of catchment coevolution. The results of this study could also be useful to facilitate evaluation of the water balance in data-scarce regions, as they help constrain parameterizations for hydrological models *a priori* using the Budyko curve as a predictor.

1 Introduction

Reliable *a priori* estimates of the catchment water balance based on minimum data requirements still represents the holy grail for many hydrologists (Sivapalan, 2003). Budyko (1974) postulated a framework to address exactly this issue, based on a top-down estimate of the steady state energy and water balance of hydrological systems. By relating the normalized actual evaporative release of water vapor to the atmosphere to the corresponding normalized atmospheric demand, using rainfall supply for normalization, he observed a considerable degree of clustering around the Budyko curve. Ever since, the Budyko framework has been successfully used for catchment classification studies at continental scale (Berghuijs et al., 2014; Wagener et al., 2007), for reducing equifinality in conceptual models by constraining the catchment water balance (Gharari et al., 2014), or for verifying uncalibrated predictions of the catchment water balance using thermodynamic optimality approaches (Porada et al., 2011). Due to this widely reported success and its theoretical underpinning (Wang et al., 2015; Westhoff et al., 2016), it appeared straightforward to us to use the Budyko framework to constrain the mean water balance of data-scarce Peruvian catchments (subcatchments of Chillón and Lurín river), which contribute to the fresh water supply of the city of Lima. However, upon comparing the water balance of a gauged catchment in the region with the Budyko curve, we noticed a considerable offset. The question thus arose whether the deviation relates to poor data quality or whether they can be explained

https://doi.org/10.5194/hess-2021-174
Preprint. Discussion started: 30 March 2021

Hydrology and Earth System Sciences
Discussions

by physiographic catchment characteristics. While both climatic and physiographic factors control the steady-state water balance, evaporation itself is commonly conceptualized as either energy or water limited. Water limitation of evaporation, however, strongly relates to root zone storage supply and thus root zone storage capacity, because evaporation is two or three orders of magnitude slower than surface runoff. Root zone storage capacity determines the amount of plant-available water and can be characterized by its total storage volume as well as capillarity-related properties like the storage at field capacity held against gravity. While free soil water above field capacity feeds groundwater and ultimately streamflow, the water content between field capacity and wilting point (effective field capacity) sustains evaporation. These catchment properties controlling root zone storage and recharge capacities are co-evolutionary fingerprints of climate and the geology setting (Gentine et al., 2012; Troch et al., 2015).

Budyko-type models have long been used for studies providing empirical relationships for first-order controls of the climate (dryness) on the mean annual water balance (e.g. Ol'dekop, 1911; Schreiber, 1904). It was, however, the curve proposed by Budyko (1974) based on the analysis of over one thousand European catchments, that gained widespread attention and was used in numerous studies. Its underlying empirical equation corresponds to the geometric mean of the two aforementioned studies by Ol'dekop and Schreiber. The Budyko curve describes the mean annual evaporation ratio ($EVR = ET_a/P$) as a function of the climatic dryness index ($\phi = ET_p/P$), with mean annual actual/potential evapotranspiration ET_a/ET_p and mean annual precipitation P (all values represent long-term annual averages). The Budyko framework assumes that the macro-climate expressed by the dryness index can be used to classify and distinguish climates and biomes, and that it is a dominant control on the steady state partitioning of annual rainfall into runoff and evaporation. The Budyko framework uses a steady-state supply-demand concept, in which the two-dimensional Budyko space is bounded by the water and energy limits that represent the physical boundaries for the mean evaporation flux. The framework was developed for long timescales and large spatial scales where the macro-climate dominates and subscale variability average out. While the Budyko curve explains a significant degree of the between-catchment variance of mean water partitioning, scattering around the curve with more or less considerable offsets lead to the question of how these deviations can be explained and if they can be generalized in an extended similarity framework.

The offsets from the Budyko curve, occurring in both directions along the EVR axis, represent the combined effects of second-order controls on the mean water balance. There is broad agreement that second-order controls and potentially resulting offsets from the Budyko curve are caused by both subscale climate variability and physiographic characteristics of the catchment. For instance, Milly (1993) and Milly (1994) explored the influence of soil water storage on the annual average water balance, using a 1d vertical soil water balance model with a stochastical meteorological forcing. While Milly's approach was simplified with respect to variability of the forcing, it nevertheless explained 85 % of the variance in water balances in the contiguous USA east of the Rocky Mountains. Milly identified the dryness index, ratio of plant-available water holding capacity to annual average precipitation and number of precipitation events per year as main controls.

Another widely applied approach relies on parametric versions of a Budyko-type model, introducing a catchment-specific parameter (Choudhury, 1999; Fu, 1981). Numerous studies use these parametrized equations, relating parameter values to physiographic catchment characteristics by fitting the model to observation data (e.g., Abatzoglou and Ficklin, 2017; Bai et al., 2020; Li et al., 2018). Donohue et al. (2007) used the catchment-specific parameter to incorporate vegetation information (e.g., leaf area, photosynthetic capacity and rooting depth) in the Budyko framework in order to explain and correct offsets from the original curve. Roderick and Farquhar (2011) used the parametrized equation to investigate changing of climate conditions and catchment characteristics. Physiographic catchment characteristics that affect the water balance are nevertheless manifold and interrelated, and it thus appears inappropriate to represent those by a single parameter. Reaver et al. (2020)

https://doi.org/10.5194/hess-2021-174
Preprint. Discussion started: 30 March 2021

recently argued that these parametric Budyko equations are under-determined and thus non-unique, and concluded that their physical interpretation was rather difficult.

There is thus a need to better understand second-order controls on the long-term water balance and their relationship to the original, non-parametric Budyko curve.

Our main objective is to explore the role of specific soil characteristics in the steady-state water balance and we hypothesize that root zone storage is an important physiographic control of offsets from the Budyko curve. Instead of using a parameterized version of the Budyko framework based on a lumped parameter, we propose a modeling approach to target specific model parameters that are more relatable to physiographic characteristics of a catchment. To that end, we selected 16 catchments covering a wide range of climate and landscape settings and calibrated a simple hydrological model (HBV-type) on the long-term water balance (30 years). Specifically, we used the calibrated models to investigate how variations in total soil storage and capillary storage fraction affect offsets from the Budyko curve, and to look for similarities in terms of the storage configurations that match the Budyko curve.

2 Methods, data and model

2.1 Selection of study catchments

In order to represent a broad range of climate settings, we based our study on several publicly available datasets from around the globe. Our choice was also conditioned by the type of available data (precipitation, potential evapotranspiration and streamflow), a minimum time series length of 30 years and the degree of preprocessing (especially spatial aggregation to catchment area) to allow for a multi-catchment approach. We finally selected 16 study catchments from the three datasets listed in Table 1.

Table 1: Datasets used and references

Region	Data used	Dataset, Source	Spatial representation
Southwest Germany State of Baden-Württemberg (“BaWue”)	Precipitation	DWD-REGNIE (DWD, 2020a)	1 km grid Germany
	Pot. evapotranspiration	DWD-ET_p (DWD, 2020b)	1 km grid Germany
	Stream flow	LUBW	station data
Continental USA (“MOPEX”)	Precipitation	MOPEX (Duan et al., 2006)	catchment average
	min./max. daily temperature	MOPEX	catchment average
	Stream flow	MOPEX	catchment average
Peru, Western Andes (“Peru”)	Precipitation	PISCO (Aybar et al., 2020)	0.1° grid Peru
	min./max. daily temperature	station data (SENAMHI)	station data
	Stream flow	Stream gauge data (SENAMHI)	station data

Our goal was not to include as many catchments as possible, but to conduct a multi-catchment study focusing on 16 distinctly different catchments. Those were selected from the three datasets using the following criteria:

https://doi.org/10.5194/hess-2021-174
Preprint. Discussion started: 30 March 2021

Hydrology and Earth System Sciences
Discussions

- **A wide range of climatic dryness indices**: In order to integrate catchments covering a large climatic gradient, we selected catchments spreading over a dryness index between $\phi = 0.3$ to $\phi = 2$. For extremer dryness values such as in desert regions or in extremely humid or cold regions (e.g., polar regions), rainfall partitioning into runoff and evaporation is not expected to relate to soil water storage characteristics. In the case of the MOPEX dataset, where several catchments at similar or same dryness indices are available, we picked a random subset of catchments.
- **Catchment area**: We selected lower mesoscale catchments ranging from around 50 to 1.000 km^2. Larger catchments potentially contain climate gradients and need to be represented by more complex distributed models. This hinders identification of clear causal relations.
- **Minimum anthropogenic influence**: In line with the Budyko framework that was developed on the basis of pristine catchments, we excluded catchments with significant anthropogenic disturbance from the study. The MOPEX dataset claims that its catchments are of little anthropogenic disturbance. The BaWue catchments were drawn from a preselection where anthropogenic influences in the form of extractions or inlets were excluded. The selected headwater catchment in the Peruvian Andes is sparsely populated due to its elevation and only has a few smaller reservoirs not expected to alter the annual catchment water balance significantly.
- **A closed water balance:** We preferred catchments with a closed long-term water balance (within 5 % error), because this is a pre-condition to apply the Budyko framework and it facilitates water balance modeling.
- **No significant snow/ice dynamics:** We did not select catchments with significant snow and ice storage, to assure that water limitation is mainly controlled by storage in the root zone.

2.2 Data and preprocessing

The Budyko framework was derived empirically, and is applicable at steady state, climatological timescales at which inter-annual storage changes in the catchment become negligible. In terms of modeling input (meteorological forcing) and output (stream flow) for the study, daily data for 30 consecutive years were retrieved for each catchment to fulfil that premise. In the following we briefly outline the necessary preprocessing steps to prepare the different data sets for modelling.

2.2.1 Preparation of the BaWue dataset

The German Meteorological Service (DWD) provides 1x1 km Germany-wide raster datasets for several climatological meteorological variables, stemming for example from the interpolation of point-wise monitoring data (e.g., from rainfall gauges) or from the processing in the framework of the spatially distributed agrometeorological AMBAV-model. For the BaWue dataset, catchment averages of daily precipitation (DWD, 2020a) and potential evapotranspiration (DWD, 2020b) were derived from the corresponding raster datasets. The potential evapotranspiration estimates are essentially based on the Penman-Monteith method. Stream flow data were obtained from the environmental agency of the State of Baden-Württemberg (LUBW, 2020).

2.2.2 Preparation of the MOPEX dataset (USA)

The MOPEX dataset (Duan et al., 2006) provides complete, catchment-averaged time series of precipitation, minimum/maximum daily temperature, NOAA climatological pan evaporation as well as stream flow data for a total of 438 catchments. Since NOAA climatological pan evaporation is based on seasonal averages with the same values recurring every year, it was considered to be less suited as forcing data for a hydrological model. Instead, potential evapotranspiration was estimated based on daily minimum and maximum temperature (Samani, 2000).

2.2.3 Preparation of the Peruvian data set

SENAMHI, the Peruvian Meteorological Service provides a national gridded precipitation data product (Aybar et al., 2020). The precipitation interpolation model relies on a combination of ground-based rainfall gauges as well as remotely sensed information used to derive spatial and seasonal patterns of precipitation and cold cloud duration. The gridded PISCO data was

https://doi.org/10.5194/hess-2021-174
Preprint. Discussion started: 30 March 2021

Hydrology and Earth System Sciences
Discussions

used to calculate catchment average precipitation for the Obrajillo (P-1) catchment. Station data from the SENAMHI station "Canta" as well as a regionally calibrated Hargreaves-Samani model was used to estimate potential evapotranspiration. For the purpose of gap filling and obtaining catchment averages from the point-wise measurements, linear correlations to nearby stations as well as elevation-dependency of the temperature were made use of. Streamflow data for the Obrajillo catchment was provided by SENAMHI. For this catchment, streamflow data was available only for roughly 19 out of the 30 years of meteorological data used to compute long-term water balances.

2.3 Characteristics of selected catchments

We finally selected 16 catchments for the study, seven from Germany (IDs: "B-*x*"), eight from the US (IDs: "M-*x*") and one from Peru ("P-1"). For the sake of readability, the original catchment/stream gauge IDs from the datasets were modified. Table A-1 in Appendix A links the original catchment IDs to the newly assigned IDs used in this study. Three maps in Appendix B show the geographic locations of the catchments. Figure 1 provides an overview over catchment and climate characteristics spanned by the selected catchments. The catchments cover areas between 50 and 1000 km^2. The catchments in Baden-Württemberg in Germany cover the most humid climate settings with dryness indexes of from 0.31 to 0.77, while some of the drier MOPEX catchments, mostly due to significantly higher potential evaporation, range between 1.05 and 1.55. In all catchments, annual total precipitation exceeds 750 mm/year. The most humid catchments in Germany reach annual totals of up to 1600 mm/year. The variation of the dryness index largely stems from the higher variations in energy supply. This is reflected in the spreading of the annual potential evapotranspiration between 500 mm/year and 1350 mm/year. Potential evapotranspiration is quite evenly distributed among the catchments in Germany, whereas precipitation is more heterogenous. Figure 1 also provides the number of rainy rays per year (a rainy day is defined as P > 1 mm/d). For most catchments, the number of rainy days correlates with mean annual precipitation. However, in the Peruvian catchment (P-1) 150 rainy days occur per year, a frequency similar to the far more humid catchments in Germany. In the more arid MOPEX catchments, the number of wet days per year is generally lower ranging between 80 and 100. Catchment M-7, however, has the lowest number of rainy days, despite a total annual precipitation of 1075 mm.

Rainfall seasonality was calculated according to Walsh and Lawler (1981)

$$SI_i = \frac{1}{P_i} \sum_{j=1}^{12} \left| P_{ij} - \frac{P_i}{12} \right|, \qquad (1)$$

where P_i is annual precipitation for year i and P_{ij} is monthly precipitation for month j in year i. For the multiannual timescale the annual seasonality indexes were averaged. Rainfall seasonality is higher in the drier catchments, in particular in catchments P-1 and M-7 (Figure 1).

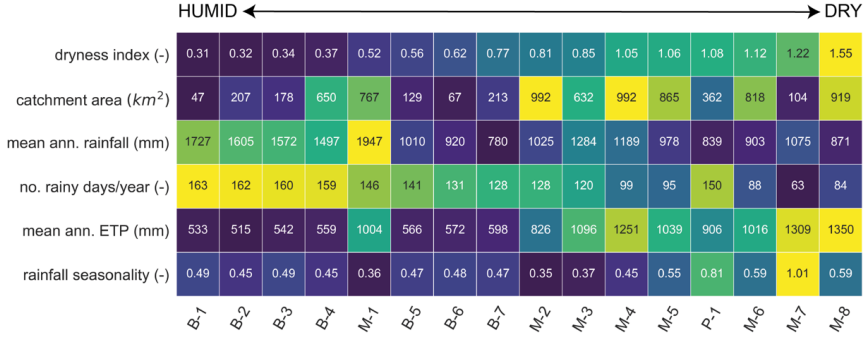

Figure 1: Overview over catchment and climate characteristics of the selected catchments (sorted by ascending dryness index). Color scale: yellow indicates high values, blue indicates low values, normalized to the range of each variable.

https://doi.org/10.5194/hess-2021-174
Preprint. Discussion started: 30 March 2021

Hydrology and Earth System Sciences
Discussions
Open Access
EGU

2.4 Hydrological modeling

The conceptual hydrological model we use for this study is a simplified version of the HBV model (Lindström et al., 1997). HBV is a widely-used hydrological model, capable of reproducing catchment dynamics across numerous hydrological settings (e.g. Booij, 2005; Osuch, 2015; Uhlenbrook et al., 1999). In the following section we explain our slightly altered and simplified derivate.

2.4.1 Conceptual model structure

Our modeling approach for the water balance is fully lumped and thus based on catchment-scale averaged values, with daily precipitation and potential evapotranspiration as meteorological forcing. The model consists of the HBV soil store to model runoff generation and actual evapotranspiration, and a single linear reservoir for daily streamflow (Figure 2).

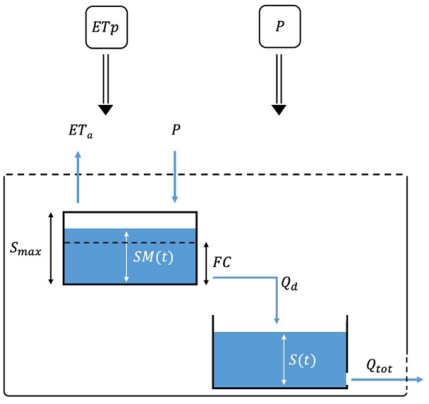

Figure 2: Setup of hydrological model. Abbreviations used for states and fluxes are explained in section 2.4.1

The soil store is characterized by the total storage volume S_{max}, its field capacity FC, and β-parameter. S_{max} corresponds to the product of effective porosity and soil depth, while FC describes the threshold below which actual evapotranspiration drops below the potential one. The water balance of the water balance of the soil bucket is:

$$\frac{dSM}{dt} = P - ET_a - Q_d \quad (2)$$

with soil water storage SM (mm), precipitation P (mm/d), actual evapotranspiration ET_a (mm/d) and direct runoff Q_d (mm/d). Direct runoff per time is calculated based on the relative saturation using a power law with β as parameter (Eq. 3). The remaining water infiltrates, and feeds evapotranspiration, while direct runoff goes to the linear reservoir:

$$Q_d = \left(\frac{SM}{S_{max}}\right)^{\beta} \cdot P \quad (3)$$

Actual evapotranspiration is a linear function of soil moisture SM below FC as given by Eq. (4) and (5):

$$ET_a = \left(\frac{SM}{FC}\right) \cdot ET_p \quad \text{f.} \quad \text{SM} < \text{FC} \quad (4)$$

$$ET_a = ET_p \quad \text{f.} \quad \text{SM} \geq \text{FC} \quad (5)$$

Contrary to the usual reservoir series used in the original HBV model, we use a single linear reservoir to simulate streamflow. It is characterized by a recession constant k_{res} (1/d) and its reservoir storage S(t), as described by Eq. (6):

$$Q_{tot} = k_{res} \cdot S \quad (6)$$

https://doi.org/10.5194/hess-2021-174
Preprint. Discussion started: 30 March 2021

This model is rather simple, but fits the purpose of annual water balance simulations (Uhlenbrook et al., 2010) and a multi-catchment approach. Here, we focus on two qualitatively different types of storage. The model accounts for the capillarity-bound storage fraction SM < FC and corresponding water limitation of evaporation, while for SM > FC evaporation is not water limited. Runoff production increases nonlinearly with SM until S_{max}. In order to characterize the relative portion of both storage fractions we define the capillary storage fraction FC_{frac} as $FC_{frac} = FC/S_{max}$.

2.4.2 Model calibration and objective functions

In order to reproduce the catchment water balance, we had to calibrate the hydrological model's parameters. Meteorological forcing data (P, ET_p) and discharge data described in section 2.2 were used to optimize the model parameters. Due to the simple fully lumped model structure and our objective to reproduce the annual water balance, the model parameters were optimized for monthly discharge values using the Kling-Gupta-efficiency (KGE) (Gupta et al., 2009) as objective function. An acceptable simulation of the water balance at the monthly scale was deemed acceptable for exploring the partitioning of rainfall into runoff and evapotranspiration at the annual and inter-annual scales. The calibration was performed on the entire datasets covering 30 consecutive years, excluding the first year as model spin-up phase. In order to make a final catchment selection based on model performance, not only monthly KGE but also the resulting mean biased water balance error (MBE) was taken into account. The MBE was calculated as given by Eq. (8), with annually aggregated streamflows, Q_i, respectively for the i-th hydrological year:

$$MBE = \frac{1}{N}\sum_{i=1}^{N}\frac{(Q_{sim,i}-Q_{obs,i})}{Q_{obs,i}} \quad (8)$$

While for the monthly KGE a threshold of 0.7 was set for acceptable model performance, a water balance error of MBE ≤ 15 % was considered sufficiently small.

We varied the four parameter β , S_{max}, FC_{frac} and k_{res} within a defined limits (Table 3) using the shuffled complex evolution SCE-UA (Duan et al., 1994) uniform sampling scheme. The parameter ranges were defined in close accordance with other studies (Beck et al., 2016; Osuch, 2015; Piotrowski et al., 2017; Wang and Solomatine, 2018).

Table 2: model parameter ranges for calibration

Parameter	Unit	Parameter limits
β	-	0.05 – 5
S_{max}	mm	50 – 800
FC_{frac}	-	0.1 – 0.9
k_{res}	1/d	0.05 – 0.9

2.4.3 Sensitivity of the water balance to soil storage parameters

We investigated the behavior of mean annual water balances across a wide range of catchments with different soil water storage properties. Therefore, the calibrated models with their optimized parameter sets were used to vary the two parameters characterizing soil water storage, S_{max} and FC_{frac} in the following within three different variation schemes:

i. Variation of S_{max} between 1 and 2000 mm in increments of ΔS_{max} = 20 mm , while the other optimized parameters (k_{res}, β and FC_{frac}) were kept constant
ii. Variation of FC_{frac} between 0.1 and 0.9 in increments of ΔFC_{frac} = 0.05, while the other optimized parameters (k_{res}, β and S_{max}) were kept constant

https://doi.org/10.5194/hess-2021-174
Preprint. Discussion started: 30 March 2021

Hydrology and Earth System Sciences
Discussions

iii. Combined variation of both soil storage parameters: all possible parameter combinations of S_{max} and FC_{frac}, given the same boundaries and increments as in i. and ii.

For each parameter combination resulting from the iterative variation process, we ran a long-term simulation (30 years at a daily timestep) and calculated the mean annual evaporation ratio (EVR). Observed EVR were estimated based on the assumption that at multiannual timescales, catchment storage changes are negligible and that mean actual evaporation thus equals the difference between mean annual precipitation and mean annual observed discharge (ET_a=P - Q).

3 Results

3.1 Water balance simulations

The model performed acceptably for the selected study catchments, with monthly KGE > 0.8 and a water balance MBE within ±15 % (Figure 3). While for catchments with lower dryness indexes, the MBE is does not exceed 5 %, it is noticeably higher for the more arid ones, reaching errors close to +15 % indicating slight overestimations of the mean annual discharge.

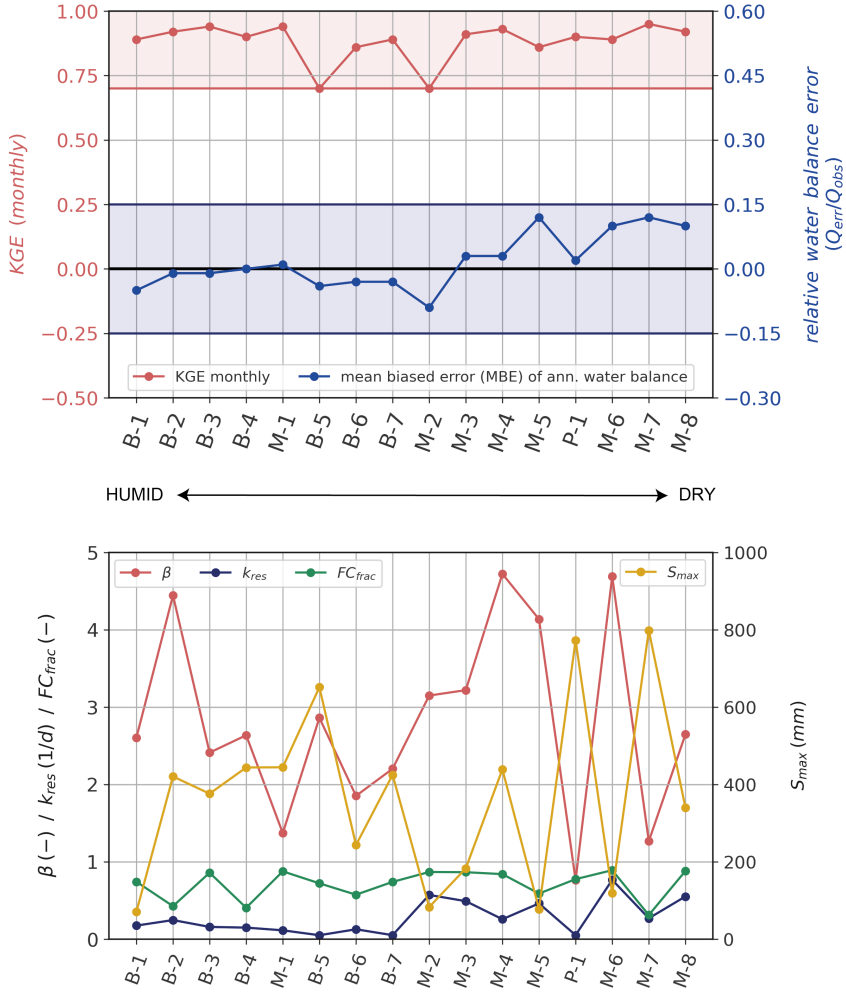

Figure 3: (top) KGE of monthly streamflow simulations and mean biased (MBE) water balance error of the calibrated models, catchments are sorted by ascending dryness. + overestimation, - underestimation. Highlighted areas: value ranges for KGE (red)

https://doi.org/10.5194/hess-2021-174
Preprint. Discussion started: 30 March 2021

and water balance (blue) with acceptable model performance. (bottom) Model parametrizations resulting from calibration of each catchment, catchments sorted by ascending dryness

The calibrated model parameters cover their predefined parameter ranges, without reaching the boundaries (Figure 3 and Table C-1 in Appendix C). The calibrated β parameters varies between 0.8 and 4.7, indicating a large spread between strong to moderate growth of area contributing to runoff with relative saturation. S_{max} ranges between 70 mm and 800 mm. Assuming a porosity of e.g. 0.4, this corresponds to an average root zone depth between 0.175 and 2 m. Field capacity ranges between 40 90 % of total root zone storage, suggesting either a rather small or strong influence of capillarity on root zone storage. The k_{res} parameter is quite uniformly distributed for the more humid catchments with values around 0.1-0.2, whereas it shows greater variability throughout the drier catchments with values between 0.26 and 0.77.

3.2 Variation of total storage volume S_{max}

The selected catchments spread across a dryness range from 0.30 to 1.55, while simulated evaporation ratios (EVR_{sim}), caused by the incremental variation of S_{max}, range between 0.05 and 0.92 (Figure 4). Generally, a higher total storage volume S_{max} corresponds a larger evaporative fraction, as visualized by the color code of the plots. At the minimal total storage volume of S_{max} = 1 mm, the catchments' evaporation ratios are around 0.1, almost independent of the dryness, as nearly 90% of the precipitation would run off. An increase in S_{max} by only 20 mm causes EVR to jump from 0.25 to 0.4. The total range of the EVR varies for the different catchments, with smaller ranges for the more humid systems, which tend to approach the energy limit at a certain point. MOPEX catchment M-7 shows the largest EVR range.

The offset from the Budyko curve is a nonlinear function of total storage volume, normalized with annual precipitation, for most study catchments (Figure 5 left). The reduction of the initially negative offsets with increasing storage shows a steep decline at small normalized storage volumes which flattens to an almost asymptotic curve at larger normalized storage volumes. This appears plausible, as the EVR is bound by the energy limit as an asymptote. When the latter is reached, the curve becomes horizontal as can be seen for the humid catchments reaching the energy limit. Exceptionally, catchment M-7 is characterized by a gradual and steady increase in EVR, with a quasilinear development up to a $S_{max}/P_{ann\text{-}avg}$ ratio of about 0.5, never really reaching this asymptotic tendency.

The EVR offset of most catchments is zero at a distinct normalized total storage volume. A comparison of these distinct total storage volumes revealed a clear clustering at 5-15 % of the annual rainfall (Figure 5 (right)). Exceptions are the Peruvian catchment P-1 as well as the U.S. catchment M-1, which do not reach the Budyko curve at all. It is also important to note that the catchment with the highest dryness index, M-8, meets the Budyko curve at a normalized total storage volume of 1.2.

https://doi.org/10.5194/hess-2021-174
Preprint. Discussion started: 30 March 2021

Hydrology and Earth System Sciences
Discussions
Open Access
EGU

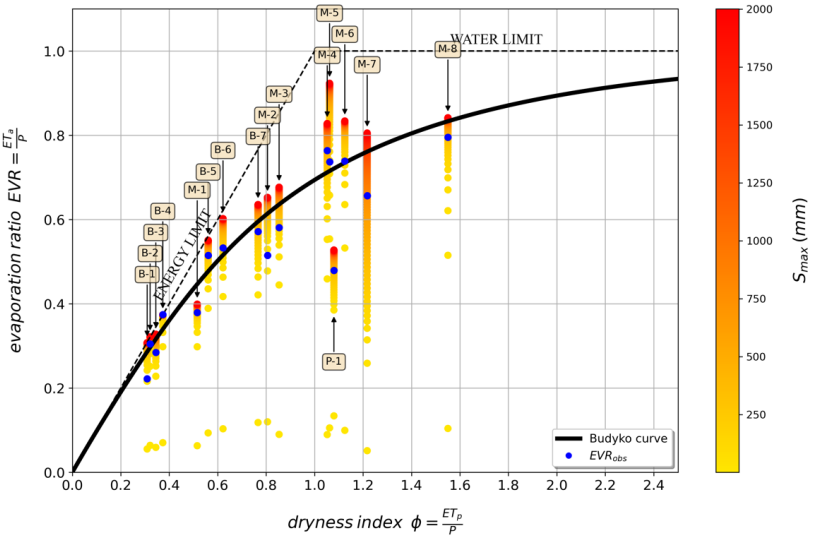

Figure 4: Variation of S_{max} in Budyko space: the simulated mean evaporation ratios (EVR) of each variation step are shown as dots. Catchment IDs indicated by arrows.

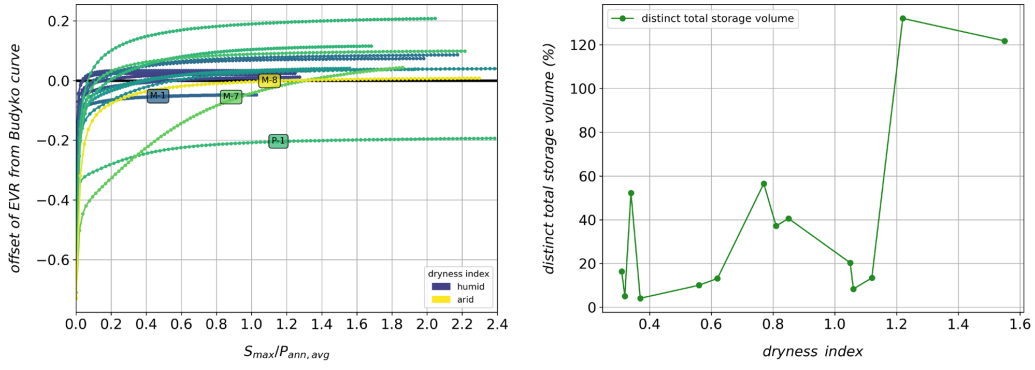

Figure 5: (left) Variation of S_{max}: offsets from Budyko curve as a function of normalized total storage. Color scale is relative to the catchments' dryness. positive values: simulated EVR higher / negative values: simulated EVR lower than Budyko curve / 0 line: EVR_{sim} matches Budyo curve. Labeled catchments are specifically addressed in the discussion. (right) distinct normalized total storage at which the catchments reach the Budyko curve as a function of the dryness index (catchments M-1 and P-1 remain below Budyko curve throughout variation of S_{max} and are thus not plotted here)

https://doi.org/10.5194/hess-2021-174
Preprint. Discussion started: 30 March 2021

Hydrology and Earth System Sciences
Discussions

3.3 Variation of the capillary storage fraction FC_{frac}

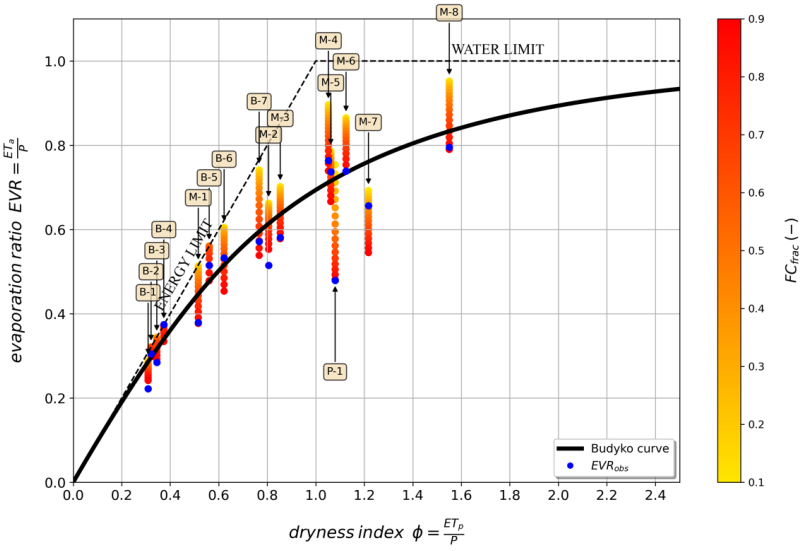

Figure 6: FC_{frac} variation in Budyko space. For each catchment the simulated mean evaporation ratios (EVR) of each variation step are visualized as one dot. Catchment IDs indicated by arrows

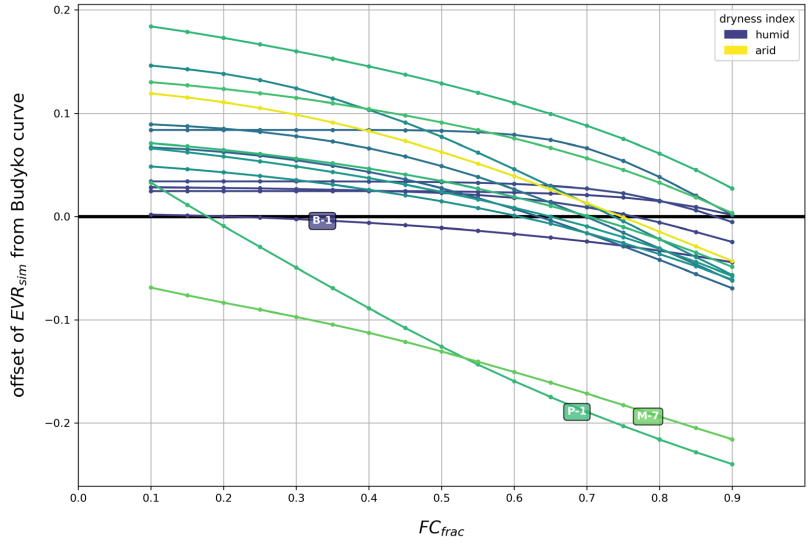

Figure 7: FC_{frac} variation, offsets from Budyko curve. Color scale is relative to the catchments' dryness indexes. positive values: simulated EVR higher / negative values: simulated EVR lower than Budyko curve / 0 line: EVR_{sim} meets Budyko curve. Labeled catchments are specifically addressed in the discussion

In the second variation scheme, the FC_{frac} model parameter was varied in [0.1, 0.9] by increments of $\Delta FC_{frac} = 0.05$, while keeping S_{max} constantly at the calibrated value. The lower the FC_{frac} parameter, the more water evaporates -being subject to water limitation in the soil- which implies higher evaporation ratios in the Budyko space (Figure 6). The total spreading of EVR is generally smaller, when compared to the variation of the total storage volume. The min-max extent of simulated EVR varies throughout the catchments, the majority of which generate EVR ranges scattering in a narrow envelope around the

https://doi.org/10.5194/hess-2021-174
Preprint. Discussion started: 30 March 2021

Budyko curve. Simulated evaporation ratios of the M-7 catchment, however, are all below the Budyko curve, while EVR for catchment M-4 remains solely above the Budyko curve. The lowest FC_{frac} values cause comparably high evaporation ratios. For humid catchments, many of those are located close to the energy limit. Catchments with dryness indices above one also reach high evaporation ratios. For instance, catchments M-8 and M-4 show simulated EVR values of around 0.9-0.95 at their lowest FC_{frac} values, which is close to the water limit.

For most catchments, the gradual increase of capillary storage fraction FC_{frac} causes a decrease in simulated EVR, which is initially quite slow at low FC_{frac} values, indicating little sensitivity in this parameter range (Figure 7). At higher FC_{frac} values of around 0.4-0.6 the reduction becomes steeper. Note that 50 % of the catchments, mostly humid ones, reach the Budyko curve at distinct capillary storage fractions clustering between 0.6 and 0.75. For another group of four catchments this distinct capillary storage fraction cluster at 0.9, which corresponds to the maximum. For two other catchments, the Peruvian P-1 and the German B-1, the distinct capillary storage fractions are around 0.2. Both show a quasilinear dependency of the evaporation ratio on FC_{frac}. The M-7 catchment, as in the previous exercise, does not reach the Budyko curve.

3.4 Simultaneous parameter variation

The simultaneous variation of the total storage volume and capillary storage fraction revealed three main types of 2-dimensional Budyko offset and EVR sensitivity pattern. Each type is visualized using representative catchments in Figure 8.

- **Type 1: humid, close to energy limit**

  Almost all parameter combinations result in an evaporation ratio close to the Budyko curve with the exception of the minimum S_{max}: value of 1mm).

- **Type 2: intermediate dryness, little seasonality**

  There is a parameter domain whose combinations result in an evaporation ratio close to the Budyko curve (hereinafter referred to as “Budyko domain”, with EVR offsets within ±0.05 from Budyko curve). At low FC_{frac} values, the Budyko domain is very sensitive to an increase of S_{max}, while at higher FC_{frac} values, this sensitivity is inverted. In between the two extremes, there is a transition zone with intermediate sensitivity of the Budyko domain to both sort of parameter changes. In this example, this transition zone extends from roughly 15-50 % of normalised total storage volumes and capillar storage fractions between 0.55-0.8 (see yellow square in Figure 8).

- **Type 3: dry (ϕ>1) catchments with pronounced seasonality**

  The two catchments with stronly seasonal climate M-7 and P-1 revealed similar EVR patterns. The Budyko domain is reached for normalized total storage volumes of more than 60 % and even 90 % of annual rainfall, respectively, at comparably low capillary storage fractions comprised between 0.1-0.4.

https://doi.org/10.5194/hess-2021-174
Preprint. Discussion started: 30 March 2021

Hydrology and Earth System Sciences
Discussions

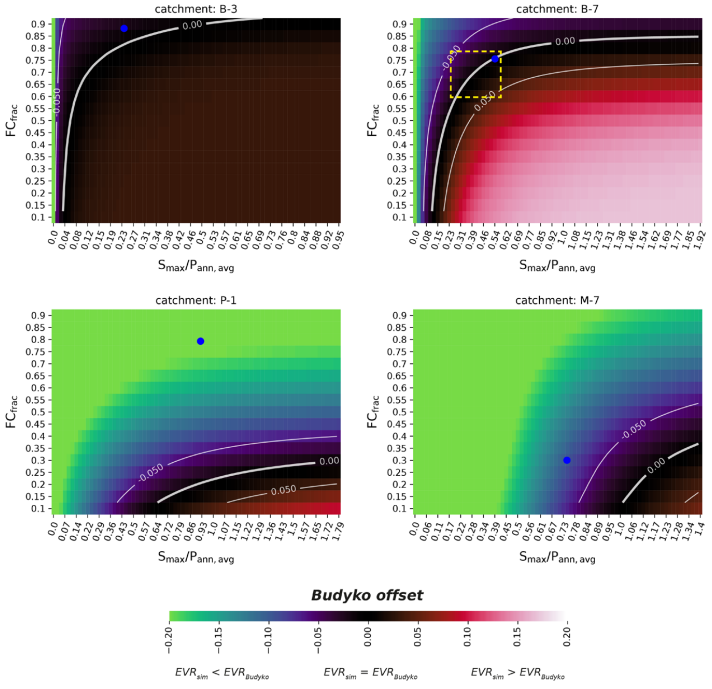

Figure 8: Simultaneous parameter variation. Simulated EVR is visualized in terms of its offset from the Budyko curve (only offsets ΔEVR < ±0.2 are sensitive to color scale). Contour lines delineate parameter combinations causing mean EVR within ±0.05 range around Budyko curve ("Budyko domain"). Blue dots: calibrated parameter combination. Yellow square: highlights a parameter subspace where catchment could evolve inside the Budyko domain with both parameters changing only moderately. Three catchment groups with distinguishable patterns emerged: (1) upper left: quite humid, close to energy limit / (2) upper right: intermediate dryness, no seasonality / (3) lower two: drier catchments with pronounced seasonality.

4 Discussion

In this study, we used a conceptual hydrological model to conduct a systematic variation of two soil storage-related parameters (S_{max}, FC_{frac}) for selected catchments across a variety of climate and landscape settings. The main goal was to investigate their role as second-order controls on the steady-state catchment water balance and in particular their suitability to explain offsets from the Budyko curve.

We start our discussion with the performance of the water balance modeling, the calibrated parameterizations, and the implications of the approach taken for the presented results. Secondly, we reflect on the sensitivity of the water balance to soil storage variations, and the related findings for different groups of catchments. Thirdly, we discuss the relative offsets from the Budyko curve, and the clustering we found in the distinct soil characteristics for matching the Budyko curve. Finally, we interpret our results in terms of catchment coevolution in the Budyko framework, concentrating on patterns that emerged during the simultaneous parameter variations.

4.1 Water balance modeling

4.1.1 Model performance and hydrologic processes representation

The hydrological model, despite its simplicity, proved capable of reproducing monthly discharge dynamics as well as the catchments' annual and interannual water balance in the 30 years of simulation period. The usefulness of similar HBV model versions for simulating discharge and water balance dynamics has been shown throughout numerous studies at comparable spatio-temporal scales (e.g. Lindström et al., 1997; Osuch et al., 2015; Seibert, 1999; Uhlenbrook et al., 2010). The performance of the model was slightly inferior for more arid catchments, perhaps due to more interannual variability in the

https://doi.org/10.5194/hess-2021-174
Preprint. Discussion started: 30 March 2021


Hydrology and Earth System Sciences
Discussions

annual water balances (and potentially also the rainfall-runoff mechanisms), which is more likely in drier climates (Koster and Suarez, 1999).

The hydrological model conceptualizes and simplifies hydrological processes. The chosen modeling approach is primarily focused on catchments where soil water storage plays a crucial role in the partitioning of rainfall into runoff and evapotranspiration, which includes a large number of catchments around the globe. For other settings, e.g., with considerable impact of snow cover or Hortonian overland flow, the dominant processes would not be well represented by the model used for this study. On the other hand, our soil storage-based reasoning is not as relevant for these types of catchments, since the water partitioning is conditioned by influences not related to soil storage volumes. Other processes that are not explicitly modelled include soil moisture redistribution due to percolation and capillary rise, and the effective cutting of evapotranspiration below the permanent wilting point. The effects of these processes on the water balance, however, are potentially compensating, depending on the individual conditions in a catchment. While percolation into deeper layers and the introduction of a permanent wilting point are likely to reduce evapotranspiration, capillary rise would rather increase evapotranspiration. The successful calibration suggests that the model yields robust estimates of mean annual water partitioning, the lack of process detail notwithstanding. The simple hydrological model we used thus seemed adequate for the main purpose of the study.

4.1.2 Catchment parametrizations and parameter interrelations

The hydrological setting of the studied catchments is represented by their calibrated parameter combinations. We found notable variability in the calibrated parameterizations not only between the three global regions, but also among the catchments within one region, for example in the geographically limited region of Baden-Württemberg in Germany (B-*x*). The catchments thus cover a range of relevant conditions, while the limited number allowed us to keep track of more detailed characteristics of each catchment. The systematic selection helped us explore the influence of storage volume-related parameters on mean hydrologic partitioning and their relationship to the Budyko curve for different hydroclimates and catchments in a more direct way than it would have been possible in a statistical analysis on an unsystematic collection including as many catchments as possible. Nonetheless, the selection of catchments is limited, and does not cover all possible meteorological forcings and hydrologic responses. For instance, the drier regimes used in this study have climates with high potential evapotranspiration. The datasets and the selection process did not yield any catchments in the dry regime with low annual precipitation (cf. section 2.3). Including such catchments in future studies would show if additional variability in the calibrated parameterizations would also increase the sensitivity to the subsequent parameter variation conducted on that basis.

In this regard, the issue of parameter correlation also needs to be addressed. The calibration results show strongly contrasted β and S_{max} values for the drier catchments included in the study, suggesting that the interplay of the two parameters affects the monthly (monthly KGE calibration) and thus likely also the annual water balances. Evidently, also total root zone storage capacity and its field capacity are closely related, as both increase with increasing fraction of silt and clay in the soil. This naturally implies that the model parameters S_{max} and FC_{frac} are interrelated as well and interact with respect to the sensitivity to EVR (Figure 8). The separate variation of both parameters yields, nevertheless, information about their relative importance in controlling EVR. The significantly larger EVR ranges in the results showed that total storage capacity dominated against the subdivision of the total storage volume in free and capillary controlled fractions. The simultaneous variation of both parameters provides a better understanding of the interactions and helps to infer distinct combinations that match the Budyko curve and find behavioral parameter sets (Schaefli et al., 2011).

https://doi.org/10.5194/hess-2021-174
Preprint. Discussion started: 30 March 2021

Hydrology and Earth System Sciences
Discussions

4.2 The role of soil storage characteristics for the evaporation ratio

4.2.1 Variation of the total storage volume

Soil water storage hydrologically acts as a control for direct runoff generation and it buffers water to feed the much slower evapotranspiration process from intermittent rainfall. When storage capacity increases, the soil is less likely to be water-saturated, leading to a higher saturation deficit and thus infiltration potential ($1 - (SM/S_{max})^{\beta}$) during rainfall events. This causes an increased water stock in the root zone which feeds evapotranspiration. In the extreme case of zero soil storage capacity, corresponding to impervious soil surface, nearly all precipitation would run off as overland flow, and the EVR would tend to zero. This is also shown by the low evaporation ratios in the corresponding simulations with the lowest S_{max} value of 1 mm. When S_{max} was increased from the minimum to small and moderate values, water partitioning was very sensitive to changes in total soil storage capacity, with evaporation ratio ranges ΔEVR from 0.1 to 0.3 for most catchments. The observed variations in sensitivities among the catchments, however, suggests additional controls on the EVR resulting from the interplay of the meteorological forcing and the parametrization.

A correlation analysis revealed that the number of rainy days per year explains 93 % of the variability in the total EVR ranges (beyond minimal $S_{max} = 1$ mm) that occurred during the variation of total storage volumes (Figure 9). Interestingly, the catchment M-7 with the highest EVR range of ΔEVR = 0.6, is characterized by a comparably small number of rainy days, which indicates, given the total rainfall amount, rather intense rainfall events (catchment characteristics in Figure 1). This is in line with Milly (1994), who found that the number of rainy days is a sensitive variable in terms of the role of soil storage and for the mean annual water balance. The lower the number of rainy days, the higher the mean rainfall depth of the events, the more storage and infiltration capacity a soil requires to retain the water and expose it to the atmospheric demand for evaporation.

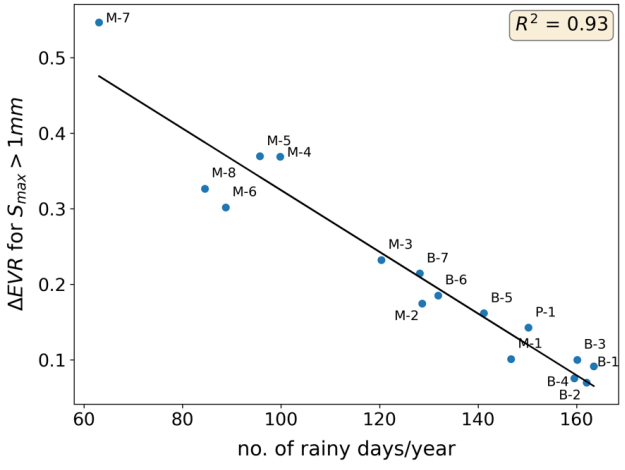

Figure 9: Linear correlation between the no. of rainfall days/year and the evaporation range (ΔEVR) spanned by the variation of S_{max} (excluding its minimum value of S_{max}=1 mm)

For almost all catchments, the sensitivity to further increase of storage capacity vanished beyond a critical normalized total storage volume, with negligible to no changes in mean evaporation (see Figure 5). For humid, energy-limited systems, a further increase of total soil storage cannot increase evapotranspiration anymore, once the energy limit is reached. The other systems reach this quasi-asymptotic behavior when two competing soil moisture influences are balanced in the model. On the one hand, a further increase of S_{max} leads to a lower relative saturation, causing a higher infiltration potential and thus providing more water for subsequent evaporation. On the other hand, this decrease of relative soil moisture leads to an increasing reduction of

https://doi.org/10.5194/hess-2021-174
Preprint. Discussion started: 30 March 2021

the evaporation flux (imitating capillary forces), which in turn retains moisture longer in the soil and limits further decrease of soil moisture. The critical S_{max} value for reaching this behavior depends on forcing characteristics and parametrization. Catchment M-7, characterized by an exceptionally low number of rainy days per year, does not reach this near-asymptotic behavior within the bounds of the S_{max} variation, again underlining the aforementioned influence of rainfall frequency on the importance of total water storage volume regarding mean annual partitioning. This finding is again in line with Milly (1994), who found a maximum value of water-holding capacity, beyond which mean evapotranspiration does no longer increase significantly.

4.2.2 Variation of the capillary storage fraction in soil

The mean annual water balance was also sensitive to changes of the capillary storage fraction of the soil, FC_{frac}, spanning EVR ranges of around ΔEVR=0.3 and ΔEVR=0.5 and with notable between-catchment variability reflecting different hydrologic behaviors. In general, higher FC_{frac} caused lower mean evapotranspiration ratios, because FC_{frac} determines the onset of water limited evapotranspiration. This reflects in a simplified and linearized manner the decrease in capillary matric potential and reduction of capillary supply of upper soil layers losing water to sustain evapotranspiration. The conceptual soil water balance models used by Milly (1994) and Potter et al. (2005) neglect this effect. For the most humid systems in particular, the decline in mean evaporation ratio occurs at capillary storage fractions ≥ 0.6. In these humid climate regimes, relative soil moisture tends to be high and in combination with lower capillary storage fractions, evapotranspiration occurs mostly without water limitation. With increasing FC_{frac} values, evapotranspiration is more likely to fall below the threshold to reduce evaporation, the soil retains more soil moisture and in turn enhances direct runoff production during rainfall. For other catchments, the sensitivity of mean EVR remains nearly uniform within the variation range of FC_{frac}, in particular for the two seasonal catchments (P-1 and M-7). This may be due to the fact that these drier, seasonal catchments tend to have relative soil moistures even below lower FC_{frac} values, making their mean water balance sensitive to FC_{frac} across the whole variation range.

4.3 Offsets from Budyko curve

4.3.1 Soil storage characteristics matching the Budyko curve

For most study catchments, the modelled EVR ranges intersect the Budyko curve at distinct values of S_{max} and FC_{frac}, respectively. The distinct storage parameters that made the systems reach the evaporation ratio predicted by the Budyko curve showed a clear clustering, and can be interpreted hydropedologically. For most of the systems, in particular for the humid catchments, the distinct normalized total storage that matches the Budyko curve is between 5-15 % of the mean annual precipitation. In case of a uniform annual rainfall regime this corresponds roughly to the monthly precipitation amount and to an S_{max} = 60-180 mm given a mean annual precipitation of P=1200 mm/a. When recalling that S_{max} equals the product of soil depth and porosity, and assuming porosity values of around 0.3-0.5, this suggests soil depths ranging between 120-540 mm. This is in the range of the root zone depths found in vegetated systems (Gentine et al., 2012). The distinct capillary storage fractions for matching the Budyko curve scattered between 0.18 and 0.90 of the total storage volume, which is the range to be expected for sandy and clayey soils, respectively. For half of the catchments, the distinct FC_{frac} ranged between 0.6 – 0.8, equivalent to loamy soils. There was, however, no clear trend of distinct capillary storage fractions with dryness index.

From our findings, we can conclude that soil storage characteristics are important second-order controls on the mean annual water balance, which can help explain observed offsets of catchments from the Budyko curve. The fact that some catchments did not reach the Budyko curve through independent variation of the soil storage parameters, however, also underlines that other second-order controls such as for example temporal variability and seasonality of the forcing, or their interplay with soil storage, can play an important role for hydrologic partitioning. Among our catchments, the two drier and in particular seasonal catchments, P-1 and M-7, stand out in this respect. While Fu and Wang (2019) show that seasonality can indeed have a

https://doi.org/10.5194/hess-2021-174
Preprint. Discussion started: 30 March 2021

significant influence on the position in the Budyko space, Potter et al. (2005) pointed out in his study on Australian catchments, that seasonality by itself was not able to explain the inter-catchment variance in the observed mean evaporation ratio.

Another possibility is that a catchment's evapotranspiration can be transport-limited when the vapor pressure gradient in the lower boundary layer is low and the air is moisture-saturated. It is conceivable that a strongly seasonal environment presents a more favorable setting for transport limitation, since the atmosphere is more likely to be moisture-saturated when the entire annual precipitation occurs within a limited number of months during the rainy season. A straightforward supplement analysis of relative humidity data of stations in the vicinity of our study catchments revealed that mean relative humidity during the rainy season for the Peruvian catchment was around 85 %, and higher than the year-round average for all other catchments. Assuming that most of the annual evapotranspiration in the Peruvian catchment occurs during the period of abundant soil moisture storage in the rainy season, it stands to reason that transport limitation can play a role in the impediment of the mean evaporation flux. This reasoning, however, does not apply to the other seasonal catchment (M-7), where different meteorological conditions in the boundary layer (e.g., in terms of advection) might counteract or limit the potential impediment of upward transport.

4.3.2 Interpretation in terms of catchment coevolution and behavioral model parameterization

Our findings fit well into the perspective that a catchment's form and functioning are co-evolutionary (Troch et al., 2015), which also implies that the development of total storage volume and of capillary storage fraction are not independent of each other. The successive variation of the two soil storage parameters sheds light on the role of the soil formation process resulting from two weathering mechanisms. While the first one (S_{max}) represents the generation of soil storage volume, i.e., porosity, the second one (FC_{frac}) relates to the transformation of coarse to increasingly fine-grained material with higher capillary forces. Both porosity and the fraction of silt and clay increase with time (Hartmann et al., 2020).

The parameter variations corresponding to these two mechanisms resulted in opposite effects on the mean evaporation ratio. This could imply that catchments with their related soil formation processes converge towards an optimal state with regard to hydrologic partitioning. While in early stages of a catchment's evolution –probably starting far off Budyko– the development of total storage S_{max} is likely to dominate the evolution, at later stages both parameters could continue to evolve simultaneously within the Budyko domain, thus keeping water balance in a steady-state in accordance with Budyko.

The idea of finding underlying organizing principles for the steady-state hydrologic partitioning described by the Budyko curve has been addressed by multiple studies in the past (cf. Berghuijs et al., 2020). Westhoff et al. (2016) showed in a backward approach that the Budyko curve can be derived using the Maximum Power principle as a constraint. Porada et al. (2011) simulated the water balance of the 35 largest basins on Earth using the SIMBA model and inferred parameters controlling root water uptake by maximizing entropy production. Simulations were in line with the Budyko framework. Milly (1994), referring also to similar conclusions by Milly and Dunne (1994), stated that simulated threshold values of water-holding capacities, beyond which evaporation does not change significantly anymore, were in proximity to the observed ones, which lead him to hypothesize that ecosystems strive to maximize evapotranspiration. The Budyko curve could thus also represent the strategy to maximize evapotranspiration by approaching the supply and demand limit, yet not reaching them due to limiting factors such as climate variability (Berghuijs et al., 2020).

If catchments were in fact to coevolve towards an optimal state of hydrologic partitioning, it would still remain difficult to infer which stage of coevolution a catchment actually is in. The plots shown in Figure 8 can be helpful in this respect, as they connect a wide range of total storage volumes and capillary storage fractions to the resulting offsets of simulated EVR from the Budyko curve. This space represents all possible system configurations with respect to these two soil storage-related parameters, and thus which soil states a catchment might potentially go through.

We found groups of catchments emerging in terms of the "Budyko domain", which clustered with respect to their climate setting and their parameter combinations in a close range of $\Delta EVR = \pm 0.05$ around the Budyko curve. The most humid

https://doi.org/10.5194/hess-2021-174
Preprint. Discussion started: 30 March 2021

catchments are bound by a tight energy limit, and hence proximity to the Budyko curve is easier to achieve, also at lower S_{max} values. For catchments of intermediate humidity, we observed a Budyko domain stretching throughout the parameter space, with the sensitivity of one parameter to the mean water balance being strongly conditioned by the other parameter. The domain highlighted by the yellow square in Figure 8 represents a parameter subspace where both parameters could develop whilst remaining within the Budyko domain. A catchment in that subset could evolve at "moderate pace" in terms of soil storage, while the water balance partitioning in terms of the Budyko framework would roughly remain constant. In the drier range of catchments, the two seasonal ones (P-1, M-7) are of particular interest. In both cases, the Budyko evaporation ratio is only reached at high S_{max} values and low FC_{frac} values. According to observed discharges and precipitation data, both are currently not inside the Budyko domain. Troch et al. (2015) introduced catchment forming factors (CFF), as quasi-independent drivers (boundary conditions) of catchment coevolution: climate, bedrock weatherability, tectonics and time, and discussed the concept of hydrologic age as the result of their combined effect. The latter is related to the amount of energy that has flown through the catchment and to the amount of physical work expended thereby. In this context one might speculate that catchments' hydrologic aging in a highly seasonal climate is slower than in humid settings. The two dryness defining variables (P, ET_p) and their corresponding mediators – water and energy – are interacting simultaneously only during 4-6 months during the rainy season, which could lead to a slower evolution towards the Budyko state in these catchments. Fu and Wang (2019) showed a positive correlation between runoff coefficients and rainfall seasonality for a number of catchments, and that such seasonal catchments tend to yield evaporation ratios below the Budyko curve, which supports this point of view.

Our results illustrate the importance of soil storage volume characteristics for the position of a catchment in the Budyko space. When making model-based predictions or when assessing the water balance in ungauged basins, the Budyko curve can be used as a landmark for long-term simulations. Schaefli et al. (2011) and Li et al. (2014) both used the Budyko curve to determine "behavioral" parameter combinations. In a similar manner, if taking potential deviations due to soil storage volume into account, model parameterizations could be oriented and constrained based on the behavior of the "Budyko domains" identified in section 3.4 for different climate types. Doing that, one could take into consideration that in catchments with high soil storage capacity, the actual water balance might exceed the evaporation ratio given by Budyko, or vice versa for catchments with little soil storage capacity (below 5-10 % of mean annual precipitation in humid climates). For example, highly erosive terrains with a steep topography could present a setting where soil storage is underdeveloped. Further research is needed, however, to address potential other second-order influences and their relative importance in comparison to soil storage characteristics for explaining offsets from the Budyko curve.

5 Conclusions

The attempt to use the empirical Budyko curve to evaluate observed water balances or to constrain them in modeling in data-scarce regions motivated us to better understand second-order controls on the steady-state water balance and potentially resulting offsets from the Budyko curve. To that end, we conducted a model study to explore the relationship between two parameters related to the soil storage volume and the Budyko curve. The modeling approach was built on observation data (P, ET_p, Q) and thus did not purely take place in the realm of simulations. The fully-lumped and simple hydrological model, similar to the widely used HBV model, proved to be an effective and efficient tool to simulate multiple catchment water balances at scales between 50-1000 km^2. Instead of using parametrized Budyko models based on a lumped parameter integrating all physiographic catchment characteristics, our study singles out specific root zone characteristics, namely total soil storage volume and the capillary storage fraction. This approach allows to relate them to tangible catchment properties and judge their physical meaningfulness.

We show the important role of soil storage as second-order controls on the mean annual water balance and potential offsets from the water balance predicted by the Budyko curve. In most cases, the parameter variations generated evaporation ratio envelopes enclosing the Budyko curve; in a few cases the Budyko curve was not reached through the variations. As suggested

https://doi.org/10.5194/hess-2021-174
Preprint. Discussion started: 30 March 2021

by other studies, the number of rainy days per year appeared to be a sensitive climate characteristic in the role soil storage plays for the water balance. We observed a clustering in terms of normalized soil storage required to match the Budyko curve at around 5-15 % of mean annual precipitation, which translates roughly to the monthly precipitation, and which reasonably corresponds to soil storage capacities commonly found in nature. Similarly, also the second parameter (capillary storage fraction) clustered in a range that agrees well with hydropedological interpretation.

Not unexpectedly, some catchments deviated from the behavior of the other catchments. In particular, the two strongly seasonal catchments, among them the Peruvian one, stood out repeatedly in the course of the analysis. Thus, while the soil storage characteristics are likely to be part of the reason for the significant offset found in the observation data of the Peruvian catchment, other second-order influences seem to be of importance as well. Several potential explanations for the deviating behavior of the seasonal catchments were elaborated, from transport limitation due to prevailing atmospheric moisture conditions to a coevolution-based argument that these catchments are still evolving towards the Budyko state. Given the outstanding role seasonal catchments played in our study, it would be interesting to conduct further research regarding the different mechanisms how precipitation seasonality (and in combination also runoff seasonality) can influence the position in the Budyko space.

In terms of potential applications, the results of this study could be helpful in the evaluation of water balances in data-scarce regions, if soil storage volumes are known to be particularly limited or, inversely, particularly abundant in a catchment. Analysis of climate type-dependent patterns of two-dimensional parameter spaces and the relative position of the Budyko domain can help provide parameter constraints for hydrological models.

Author contributions

Jan Bondy conceptualized the study, conducted the analysis and wrote the paper. Jan Wienhöfer provided insights into interpretation and discussion, and improved the structure of the paper. Laurent Pfister contributed with discussions on the Budyko framework and helped shape the final manuscript. Erwin Zehe conceived of the general idea and supervised the study.

Acknowledgements

We thank Sophia Peschko-Ziesak for her work in the preselection of catchments/stream gauges in Baden-Württemberg. We also want to thank SENAMHI, the Peruvian Meteorological and Hydrological Service, for providing both rainfall and discharge data for Peruvian catchments.

Competing interests

The authors declare that they have no conflict of interest.

6 References

Abatzoglou, J. T. and Ficklin, D. L.: Climatic and physiographic controls of spatial variability in surface water balance over the contiguous United States using the Budyko relationship, Water Resour. Res., 53(9), 7630–7643, https://doi.org/10.1002/2017WR020843, 2017.

Aybar, C., Fernández, C., Huerta, A., Lavado, W., Vega, F. and Felipe-Obando, O.: Construction of a high-resolution gridded rainfall dataset for Peru from 1981 to the present day, Hydrol. Sci. J., 65(5), 770–785, https://doi.org/10.1080/02626667.2019.1649411, 2020.

Bai, P., Liu, X., Zhang, D. and Liu, C.: Estimation of the Budyko model parameter for small basins in China, Hydrol. Process., 34(1), 125–138, https://doi.org/10.1002/hyp.13577, 2020.

Beck, H. E., Dijk, A. I. J. M. van, Roo, A. de, Miralles, D. G., McVicar, T. R., Schellekens, J. and Bruijnzeel, L. A.: Global-scale regionalization of hydrologic model parameters, Water Resour. Res., 52(5), 3599–3622, https://doi.org/10.1002/2015WR018247, 2016.

https://doi.org/10.5194/hess-2021-174
Preprint. Discussion started: 30 March 2021

Hydrology and Earth System Sciences
Discussions

Berghuijs, W., Woods, R. and Gnann, S.: Unanswered questions on the Budyko framework, Hydrol. Process., https://doi.org/10.1002/hyp.13958, 2020.

Berghuijs, W. R., Sivapalan, M., Woods, R. A. and Savenije, H. H. G.: Patterns of similarity of seasonal water balances: A window into streamflow variability over a range of time scales, Water Resour. Res., 50(7), 5638–5661, https://doi.org/10.1002/2014WR015692, 2014.

Booij, M. J.: Impact of climate change on river flooding assessed with different spatial model resolutions, J. Hydrol., 303(1), 176–198, https://doi.org/10.1016/j.jhydrol.2004.07.013, 2005.

Budyko, M. I.: Climate and Life, Academic Press, Inc. http://ndl.ethernet.edu.et/handle/123456789/43846, last access: 14 October 2020, 1974.

Choudhury, BhaskarJ.: Evaluation of an empirical equation for annual evaporation using field observations and results from a biophysical model, J. Hydrol., 216(1), 99–110, https://doi.org/10.1016/S0022-1694(98)00293-5, 1999.

Donohue, R., Roderick, M. and McVicar, T. R.: On the importance of including vegetation dynamics in Budyko's hydrological model, Hydrol. Earth Syst. Sci. https://openresearch-repository.anu.edu.au/handle/1885/39405, last access: 17 November 2020, 2007.

Duan, Q., Sorooshian, S. and Gupta, V. K.: Optimal use of the SCE-UA global optimization method for calibrating watershed models, J. Hydrol., 158(3), 265–284, https://doi.org/10.1016/0022-1694(94)90057-4, 1994.

Duan, Q., Schaake, J., Andréassian, V., Franks, S., Goteti, G., Gupta, H. V., Gusev, Y. M., Habets, F., Hall, A., Hay, L., Hogue, T., Huang, M., Leavesley, G., Liang, X., Nasonova, O. N., Noilhan, J., Oudin, L., Sorooshian, S., Wagener, T. and Wood, E. F.: Model Parameter Estimation Experiment (MOPEX): An overview of science strategy and major results from the second and third workshops, J. Hydrol., 320(1), 3–17, https://doi.org/10.1016/j.jhydrol.2005.07.031, 2006.

DWD: DWD Climate Data Center (CDC), REGNIE-Raster der täglichen Niederschlagshöhe für Deutschland, 2020a.

DWD: DWD Climate Data Center (CDC): Tägliche Raster der potentiellen Evapotranspiration über Gras, Version 0.x, 2020b.

Fu, B.: On the calculation of the evaporation from land surface, Atmos Sin, 5, 23–31, 1981.

Fu, J. and Wang, W.: On the lower bound of Budyko curve: The influence of precipitation seasonality, J. Hydrol., 570, 292–303, https://doi.org/10.1016/j.jhydrol.2018.12.062, 2019.

Gentine, P., D'Odorico, P., Lintner, B. R., Sivandran, G. and Salvucci, G.: Interdependence of climate, soil, and vegetation as constrained by the Budyko curve, Geophys. Res. Lett., 39(19), https://doi.org/10.1029/2012GL053492, 2012.

Gharari, S., Hrachowitz, M., Fenicia, F., Gao, H. and Savenije, H. H. G.: Using expert knowledge to increase realism in environmental system models can dramatically reduce the need for calibration, Hydrol. Earth Syst. Sci., 18(12), 4839–4859, https://doi.org/10.5194/hess-18-4839-2014, 2014.

Gupta, H. V., Kling, H., Yilmaz, K. K. and Martinez, G. F.: Decomposition of the mean squared error and NSE performance criteria: Implications for improving hydrological modelling, J. Hydrol., 377(1), 80–91, https://doi.org/10.1016/j.jhydrol.2009.08.003, 2009.

Hartmann, A., Weiler, M. and Blume, T.: The impact of landscape evolution on soil physics: evolution of soil physical and hydraulic properties along two chronosequences of proglacial moraines, Earth Syst. Sci. Data, 12(4), 3189–3204, https://doi.org/10.5194/essd-12-3189-2020, 2020.

Koster, R. D. and Suarez, M. J.: A Simple Framework for Examining the Interannual Variability of Land Surface Moisture Fluxes, J. Clim., 12(7), 1911–1917, https://doi.org/10.1175/1520-0442(1999)012<1911:ASFFET>2.0.CO;2, 1999.

Li, C., Wang, L., Wanrui, W., Qi, J., Linshan, Y., Zhang, Y., Lei, W., Cui, X. and Wang, P.: An analytical approach to separate climate and human contributions to basin streamflow variability, J. Hydrol., 559, 30–42, https://doi.org/10.1016/j.jhydrol.2018.02.019, 2018.

Lindström, G., Johansson, B., Persson, M., Gardelin, M. and Bergström, S.: Development and test of the distributed HBV-96 hydrological model, J. Hydrol., 201(1–4), 272–288, https://doi.org/10.1016/S0022-1694(97)00041-3, 1997.

LUBW: Pegel-und Datendienst, 2020.

https://doi.org/10.5194/hess-2021-174
Preprint. Discussion started: 30 March 2021

Milly, P. C. D.: An analytic solution of the stochastic storage problem applicable to soil water, Water Resour. Res., 29(11), 3755–3758, https://doi.org/10.1029/93WR01934, 1993.

Milly, P. C. D.: Climate, soil water storage, and the average annual water balance, Water Resour. Res., 30(7), 2143–2156, https://doi.org/10.1029/94WR00586, 1994.

Milly, P. C. D. and Dunne, K. A.: Sensitivity of the Global Water Cycle to the Water-Holding Capacity of Land, J. Clim., 7(4), 506–526, https://doi.org/10.1175/1520-0442(1994)007<0506:SOTGWC>2.0.CO;2, 1994.

Ol'dekop, E. M.: On Evaporation From the Surface of River Basins, Lurevskogo Univ Tartu Est., Collection of the Works of Students of the Meteorological Observatory, 1911.

Osuch, M.: Sensitivity and Uncertainty Analysis of Precipitation-Runoff Models for the Middle Vistula Basin, in Stochastic Flood Forecasting System: The Middle River Vistula Case Study, edited by R. J. Romanowicz and M. Osuch, pp. 61–81, Springer International Publishing, Cham, https://doi.org/10.1007/978-3-319-18854-6_5, , 2015.

Osuch, M., Romanowicz, R. J. and Booij, M. J.: The influence of parametric uncertainty on the relationships between HBV model parameters and climatic characteristics, Hydrol. Sci. J., 60(7–8), 1299–1316, https://doi.org/10.1080/02626667.2014.967694, 2015.

Piotrowski, A. P., Napiorkowski, M. J., Napiorkowski, J. J., Osuch, M. and Kundzewicz, Z. W.: Are modern metaheuristics successful in calibrating simple conceptual rainfall–runoff models?, Hydrol. Sci. J., 62(4), 606–625, https://doi.org/10.1080/02626667.2016.1234712, 2017.

Porada, P., Kleidon, A. and Schymanski, S. J.: Entropy production of soil hydrological processes and its maximisation, Earth Syst. Dyn., 2(2), 179–190, https://doi.org/10.5194/esd-2-179-2011, 2011.

Potter, N. J., Zhang, L., Milly, P. C. D., McMahon, T. A. and Jakeman, A. J.: Effects of rainfall seasonality and soil moisture capacity on mean annual water balance for Australian catchments, Water Resour. Res., 41(6), https://doi.org/10.1029/2004WR003697, 2005.

Reaver, N. G. F., Kaplan, D. A., Klammler, H. and Jawitz, J. W.: Reinterpreting the Budyko Framework, Hydrol. Earth Syst. Sci. Discuss., 1–31, https://doi.org/10.5194/hess-2020-584, 2020.

Roderick, M. L. and Farquhar, G. D.: A simple framework for relating variations in runoff to variations in climatic conditions and catchment properties, Water Resour. Res., 47(12), https://doi.org/10.1029/2010WR009826, 2011.

Samani, Z.: Estimating Solar Radiation and Evapotranspiration Using Minimum Climatological Data, J. Irrig. Drain. Eng., 126(4), 265–267, https://doi.org/10.1061/(ASCE)0733-9437(2000)126:4(265), 2000.

Schaefli, B., Harman, C. J., Sivapalan, M. and Schymanski, S. J.: HESS Opinions: Hydrologic predictions in a changing environment: behavioral modeling, Hydrol. Earth Syst. Sci., 15(2), 635–646, https://doi.org/10.5194/hess-15-635-2011, 2011.

Schreiber, P.: Über die Beziehungen zwischen dem Niederschlag und der Wasserführung der Flüsse in Mitteleuropa, Z Meterol, 21(10), 441–452, 1904.

Seibert, J.: Regionalisation of parameters for a conceptual rainfall-runoff model, Agric. For. Meteorol., 98–99, 279–293, https://doi.org/10.1016/S0168-1923(99)00105-7, 1999.

Sivapalan, M.: Prediction in ungauged basins: a grand challenge for theoretical hydrology, Hydrol. Process., 17(15), 3163–3170, https://doi.org/10.1002/hyp.5155, 2003.

Troch, P. A., Lahmers, T., Meira, A., Mukherjee, R., Pedersen, J. W., Roy, T. and Valdés-Pineda, R.: Catchment coevolution: A useful framework for improving predictions of hydrological change?, Water Resour. Res., 51(7), 4903–4922, https://doi.org/10.1002/2015WR017032, 2015.

Uhlenbrook, S., Seibert, J., Leibundgut, C. and Rodhe, A.: Prediction uncertainty of conceptual rainfall-runoff models caused by problems in identifying model parameters and structure, Hydrol. Sci. J., 44(5), 779–797, https://doi.org/10.1080/02626669909492273, 1999.

Uhlenbrook, S., Mohamed, Y. and Gragne, A. S.: Analyzing catchment behavior through catchment modeling in the Gilgel Abay, Upper Blue Nile River Basin, Ethiopia, Hydrol. Earth Syst. Sci., 14(10), 2153–2165, https://doi.org/10.5194/hess-14-2153-2010, 2010.

https://doi.org/10.5194/hess-2021-174
Preprint. Discussion started: 30 March 2021

Wagener, T., Sivapalan, M., Troch, P. and Woods, R.: Catchment Classification and Hydrologic Similarity, Geogr. Compass, 1(4), 901–931, https://doi.org/10.1111/j.1749-8198.2007.00039.x, 2007.

Walsh, R. P. D. and Lawler, D. M.: Rainfall Seasonality: Description, Spatial Patterns and Change Through Time, Weather, 36(7), 201–208, https://doi.org/10.1002/j.1477-8696.1981.tb05400.x, 1981.

Wang, A. and Solomatine, D. P.: Practical experience and framework for sensitivity analysis of hydrological models: six methods, three models, three criteria, Hydrol. Earth Syst. Sci. Discuss., 1–34, https://doi.org/10.5194/hess-2018-78, 2018.

Wang, D., Zhao, J., Tang, Y. and Sivapalan, M.: A thermodynamic interpretation of Budyko and L'vovich formulations of annual water balance: Proportionality Hypothesis and maximum entropy production, Water Resour. Res., 51(4), 3007–3016, https://doi.org/10.1002/2014WR016857, 2015.

Westhoff, M., Zehe, E., Archambeau, P. and Dewals, B.: Does the Budyko curve reflect a maximum-power state of hydrological systems? A backward analysis, Hydrol. Earth Syst. Sci., 20(1), 479–486, https://doi.org/10.5194/hess-20-479-2016, 2016.

Yang, D., Sun, F., Liu, Z., Cong, Z., Ni, G. and Lei, Z.: Analyzing spatial and temporal variability of annual water-energy balance in nonhumid regions of China using the Budyko hypothesis, Water Resour. Res., 43(4), https://doi.org/10.1029/2006WR005224, 2007.

7 Appendix

Appendix A Catchment IDs

Table A-1: Original catchment IDs and the IDs assigned in this study

Original catchment /Stream gauge ID	Catchment ID used in this paper
3303	B-1
3304	B-2
3302	B-3
2340	B-4
03443000	M-1
177	B-5
3314	B-6
478	B-7
01534000	M-2
03438000	M-3
07346050	M-4
06914000	M-5
Obrajillo	P-1
06888500	M-6
011160000	M-7
08171000	M-8

https://doi.org/10.5194/hess-2021-174
Preprint. Discussion started: 30 March 2021

Hydrology and Earth System Sciences
Discussions
Open Access
EGU

Appendix B Geographic locations of catchments

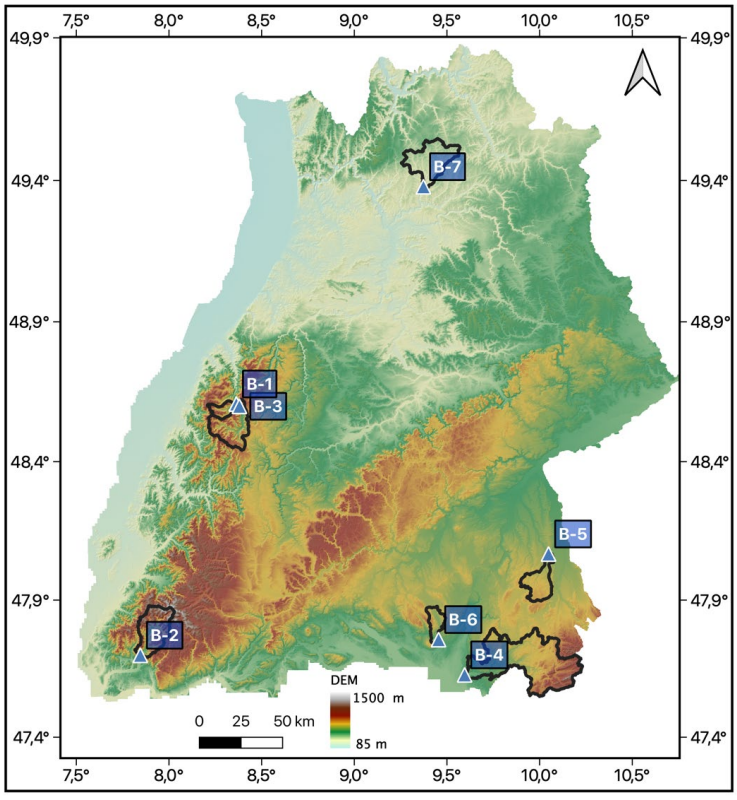

Figure B-1: Selected catchments in Baden-Württemberg, Germany

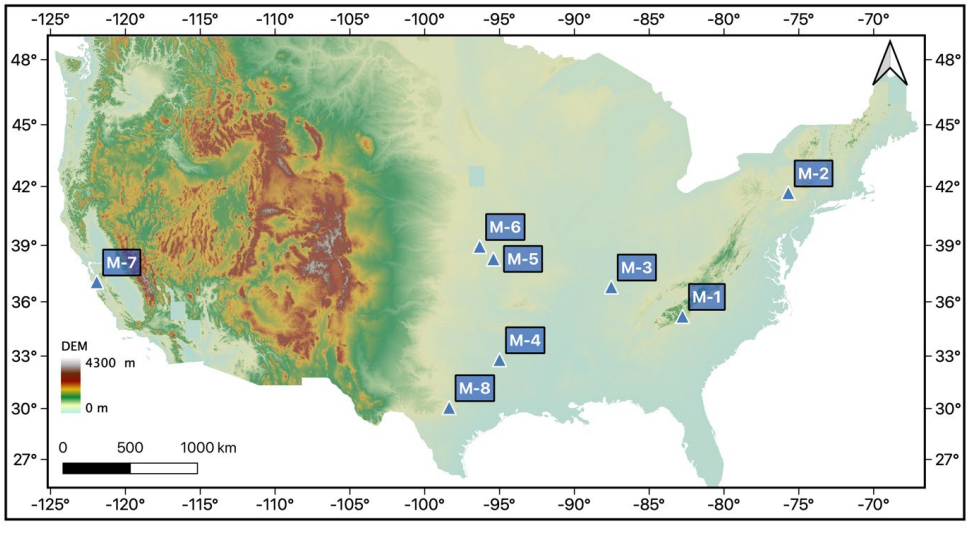

Figure B-2: Selected MOPEX catchments in USA

https://doi.org/10.5194/hess-2021-174
Preprint. Discussion started: 30 March 2021

Hydrology and Earth System Sciences
Discussions
Open Access
EGU

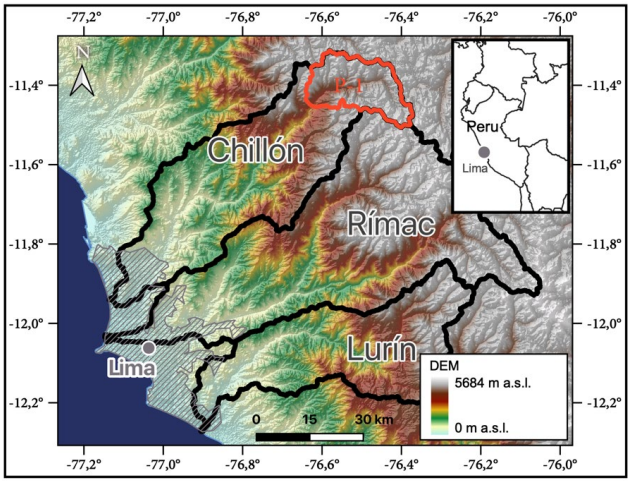

Figure B-3: Peruvian catchment P-1

Appendix C Calibrated parameters and loss functions

Table C-1: Calibrated parameters and loss functions

	beta	Kres	FC_frac	Smax	KGE_mon	MBE
B-1	2.6	0.18	0.74	70.6	0.89	-0.05
B-2	4.45	0.25	0.43	420.8	0.92	-0.01
B-3	2.41	0.16	0.86	376.2	0.94	-0.01
B-4	2.64	0.15	0.41	444	0.9	0
M-1	1.37	0.11	0.88	444.5	0.94	0.01
B-5	2.86	0.05	0.72	651.5	0.7	-0.04
B-6	1.85	0.13	0.57	243.4	0.86	-0.03
B-7	2.2	0.05	0.74	425	0.89	-0.03
M-2	3.15	0.57	0.87	83.06	0.7	-0.09
M-3	3.22	0.49	0.87	183.1	0.91	0.03
M-4	4.72	0.26	0.84	439.2	0.93	0.03
M-5	4.14	0.46	0.59	77.7	0.86	0.12
P-1	0.76	0.05	0.78	773	0.9	0.02
M-6	4.69	0.77	0.89	118.75	0.89	0.1
M-7	1.27	0.27	0.31	798.5	0.95	0.12
M-8	2.65	0.55	0.88	340.2	0.92	0.1